nana plant2 Encodes a Maize Ortholog of the Arabidopsis Brassinosteroid Biosynthesis Gene *DWARF1*, Identifying Developmental Interactions between Brassinosteroids and Gibberellins[1][OPEN]

Norman B. Best, Thomas Hartwig[2], Josh Budka, Shozo Fujioka, Gurmukh Johal, Burkhard Schulz[3]*, and Brian P. Dilkes*

Department of Horticulture and Landscape Architecture (N.B.B., T.H., J.B., B.S.), Department of Biochemistry (N.B.B., B.P.D.), and Department of Botany and Plant Pathology (G.J.), Purdue University, West Lafayette, Indiana 47907; and RIKEN Center for Sustainable Resource Science, Wako-shi, Saitama 351-0198, Japan (S.F.)

ORCID IDs: 0000-0002-6572-5999 (N.B.B.); 0000-0002-2707-2771 (T.H.); 0000-0001-5291-2763 (B.S.); 0000-0003-2799-954X (B.P.D.).

A small number of phytohormones dictate the pattern of plant form affecting fitness via reproductive architecture and the plant's ability to forage for light, water, and nutrients. Individual phytohormone contributions to plant architecture have been studied extensively, often following a single component of plant architecture, such as plant height or branching. Both brassinosteroid (BR) and gibberellin (GA) affect plant height, branching, and sexual organ development in maize (*Zea mays*). We identified the molecular basis of the *nana plant2* (*na2*) phenotype as a loss-of-function mutation in one of the two maize paralogs of the Arabidopsis (*Arabidopsis thaliana*) BR biosynthetic gene *DWARF1* (*DWF1*). These mutants accumulate the DWF1 substrate 24-methylenecholesterol and exhibit decreased levels of downstream BR metabolites. We utilized this mutant and known GA biosynthetic mutants to investigate the genetic interactions between BR and GA. Double mutants exhibited additivity for some phenotypes and epistasis for others with no unifying pattern, indicating that BR and GA interact to affect development but in a context-dependent manner. Similar results were observed in double mutant analyses using additional BR and GA biosynthetic mutant loci. Thus, the BR and GA interactions were neither locus nor allele specific. Exogenous application of GA_3 to *na2* and *d5*, a GA biosynthetic mutant, also resulted in a diverse pattern of growth responses, including BR-dependent GA responses. These findings demonstrate that BR and GA do not interact via a single inclusive pathway in maize but rather suggest that differential signal transduction and downstream responses are affected dependent upon the developmental context.

Aboveground plant form is achieved by the progressive addition of organs, which guarantees plant success through the acquisition of light and gases to support photosynthesis and reproduction. Multiple phytohormones regulate the architecture of organs, the rate at which they grow, and their placement on the growing axes of plants (Sussex and Kerk, 2001; Jaillais and Chory, 2010; Depuydt and Hardtke, 2011). This regulation not only contributes to the diversity of plant form and the adaptation of plants to their environments (Orshan, 1986; Chapin et al., 1987) but has been central to major gains in crop yield in the 20th and 21st centuries (Salamini, 2003; Salas Fernandez et al., 2009). Phytohormone regulation of plant architecture and components such as plant height, branching, and floral organ development has been studied extensively (Evans and Poethig, 1995; Choe et al., 2001; Hong et al., 2004; Sakamoto et al., 2006). The simultaneous presence of multiple phytohormones in all plant tissues raises the question: how do interactions between these developmental determinants influence the plant form? Multiple studies of gene expression demonstrated shared and distinct gene expression responses for various combinations of phytohormones in Arabidopsis (*Arabidopsis thaliana*; Nemhauser et al., 2006; Jaillais and Chory, 2010; Wang et al., 2011; Vanstraelen and Benková, 2012). However, the developmental consequences and changes in gene expression within these interactions

[1] This work was supported by the National Science Foundation (EAGER grant no. 1450341 to B.P.D. and CAREER grant no. 1054918 to B.S.).

[2] Present address: Department of Biology, Carnegie Institution for Science, Stanford, CA 94305.

[3] Present address: Department of Plant Science and Landscape Architecture, University of Maryland, College Park, MD 20742.

* Address correspondence to bschulz1@umd.edu or bdilkes@purdue.edu.

The author responsible for distribution of materials integral to the findings presented in this article in accordance with the policy described in the Instructions for Authors (www.plantphysiol.org) is: Brian P. Dilkes (bdilkes@purdue.edu).

B.P.D. and B.S. led the project; N.B.B. and B.P.D wrote the article; N.B.B. performed the transcript measurements, genomic sequencing, double mutant analysis, phytohormone treatments and analysis, and phylogenetic analysis; T.H. and J.S. assisted with material generation and genomic sequencing; S.F. performed the brassinosteroid measurements; G.J. provided genetic material and assisted with genetic aspects of the project; all authors read and revised the article.

[OPEN] Articles can be viewed without a subscription.

www.plantphysiol.org/cgi/doi/10.1104/pp.16.00399

resulting in their interdependency on plant development are largely unknown.

Brassinosteroid (BR) and gibberellin (GA) are two phytohormones that have similar effects on anisotropic cell expansion. As a result, both contribute to the directional expansion of plant organs and are involved in similar developmental processes (Santner et al., 2009; Santner and Estelle, 2009; Wolters and Jürgens, 2009; Hamant and Traas, 2010). BRs are polyhydroxylated steroidal compounds that control plant height, skotomorphogenesis and photomorphogenesis, branching, reproductive organ development, stomatal development, and disease resistance (Choe et al., 2001; Nakashita et al., 2003; Hartwig et al., 2011; Kim et al., 2012; Oh et al., 2012; Makarevitch et al., 2012; Wang et al., 2013). BR at concentrations of $N \times 10^{-10}$ is biologically active and sensitizes plants to auxin applications (Wada et al., 1981; Vert et al., 2008). BR and auxin positively regulate each other's biosynthesis (Li et al., 2005; Kim et al., 2014), resulting in a positive regulatory loop. GA also influences plant height, branching, reproductive organ development, stomatal development, and disease resistance (Evans and Poethig, 1995; Eckardt, 2002; Saibo et al., 2003; Elfving et al., 2011).

Maize (*Zea mays*) is a monoecious species, which produces two types of imperfect flowers in two distinct locations. Staminate flowers are produced at the apex of the shoot in the tassel florets, and pistillate flowers are present on lateral branches in the ear florets. In the two inflorescences, organs are arrested or aborted postinitiation to prevent their manifestation in mature florets. BR-deficient mutants in maize exhibit severe dwarfism, altered leaf morphology, and pistil production in the tassel (Hartwig et al., 2011; Makarevitch et al., 2012). Other *tasselseed* (*ts*) mutants in maize are not dwarf. The genes responsible for some of these mutants are molecularly defined. Mutants such as *ts1* and *ts2* have a proposed function in jasmonic acid (JA) metabolism (DeLong et al., 1993; Acosta et al., 2009), while other mutants are involved in encoding an APETELA2-like transcription factor, *Ts6*, as well as its corresponding microRNA, *ts4* (Chuck et al., 2007). As a result, the ability of JA to inhibit pistil production in the maize tassel has been a leading hypothesis for tassel seed production. However, work by Nickerson (1959) demonstrated that sustained GA_3 treatments of the maize growing point induced tassel seeds in multiple wild-type maize inbred backgrounds. Consonant with a role for GA in the regulation of maize floral organ persistence, mutants deficient in GA biosynthesis were unable to suppress stamen production in the ear (Emerson et al., 1935). The JA and GA effects appear to be independent, as pistil persistence in the tassel florets of the *ts1* and *ts2* mutants was not suppressed by the loss of GA synthesis in double mutants between *ts1* or *ts2* and the GA-deficient mutant *dwarf1* (*d1*; Irish et al., 1994). Thus, an overproduction of GA or a deficiency of JA in BR-deficient mutants could result in tassel seed production.

Much of what we currently know about the interactions between BR and GA is from experiments in Arabidopsis and a single seedling organ, the hypocotyl (Bai et al., 2012; Li et al., 2012; Stewart Lilley et al., 2013; Oh et al., 2014). In monocots, a study on rice (*Oryza sativa*) seedlings showed that BR and GA cross talk is dependent upon the tissue studied and the hormone concentration, exhibiting different results from Arabidopsis (Tong et al., 2014). If plants utilize nonoverlapping mechanisms to integrate signals, single-tissue studies may oversimplify their interactions and fail to explain the roles of these molecules in generating the diversity of plant adaptations and forms.

We report the characterization and cloning of *nana plant2* (*na2*), first identified by H.S. Perry in the 1930s (Emerson et al., 1935). The *na2* mutants exhibited severe dwarfism, suppression of tillers, altered leaf morphology, and a failure to suppress pistils in the tassel florets. We demonstrated that *na2* was defective in the reduction of 24-methylenecholesterol to campesterol, caused by a mutation of Δ^{24}-sterol reductase involved in BR biosynthesis. To investigate the hormonal regulation and cross talk of maize architecture, we created BR- and GA-deficient double mutants in maize. Through the analysis of these double mutants, we identified distinct genetic interactions between BR and GA mutants that were developmentally specific. GA was required for pistil production in the tassels of BR mutants, and BR was required for the increased branching observed in GA mutants, while BR and GA additively influenced plant height. Thus, the control of maize architecture by phytohormones, made visible by blocking their biosynthesis, is the result of interdependent signaling events that identify GA and BR cross talk as a critical determinant of maize development.

RESULTS

na2 Mutants Are Disrupted in the Δ^{24}-Sterol Reductase of Maize

The maize line 4407D d*-N2374 was identified as an extreme dwarf among images of maize mutants (http://maizegdb.org/cgi-bin/displayvarrecord.cgi?id=75364). Figure 1 shows the phenotypes displayed by greenhouse-grown plants from this line, including dwarfism, feminized tassels, reduced branching, and upright leaves. Many of these are shared by the BR biosynthetic mutant *na1* (Hartwig et al., 2011). Crosses between *na1-1* and line 4407D d*-N2374 complemented these phenotypes to the wild type in the F1 generation, demonstrating that the 4407D d*-N2374 mutant defined a distinct locus. To test allelism between 4407D d*-N2374 and the classical mutant *na2* (Emerson et al., 1935), homozygous mutant pollen parents were crossed to heterozygous ear parents. 4407D d*-N2374 failed to complement the *na2* phenotypes in two stocks bearing mutations in *na2*, the *na2-506D* line and *na2-518C* introgressed into Hi27, demonstrating that line 4407D d*-N2374 is a new allele of *na2* (wild type:*na2*, 73:57 [χ^2 $P = 0.22$]

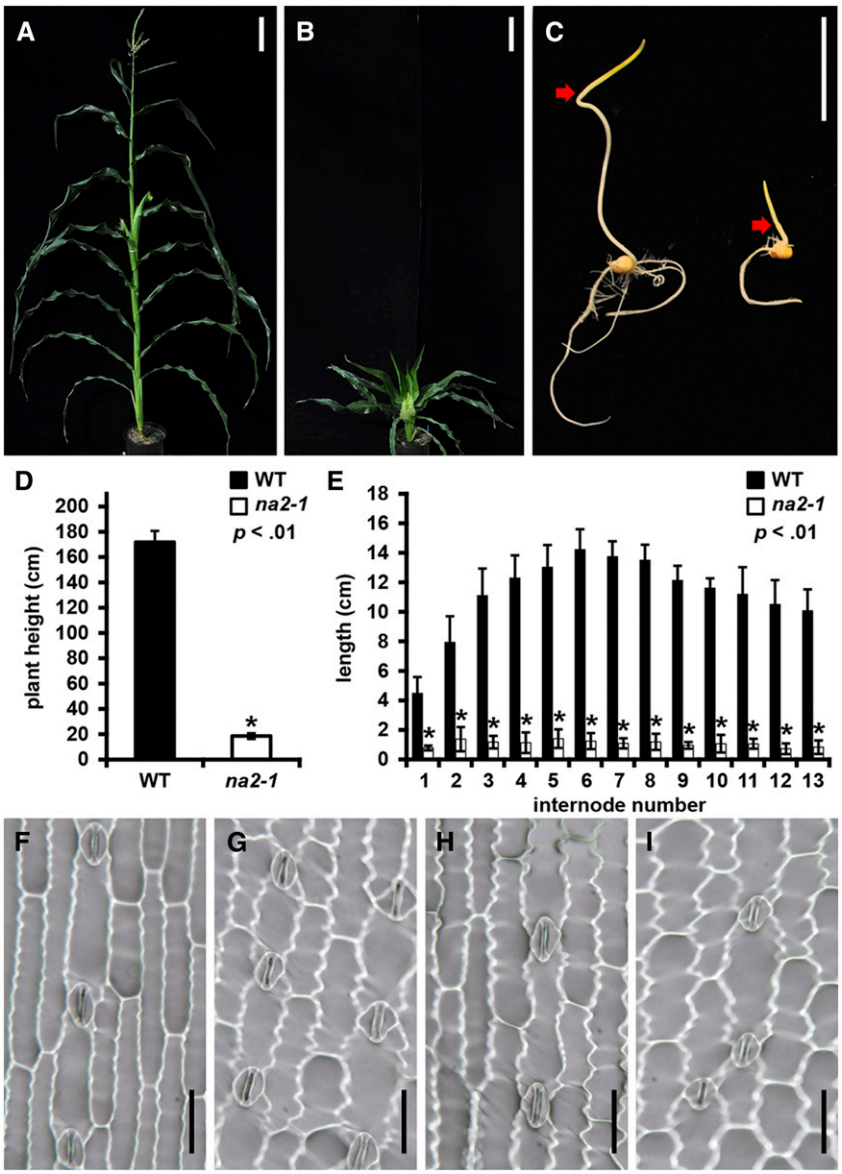

Figure 1. Morphological features of *na2* mutants. A, Mature wild-type plant. B, *na2-1* plant. C, Wild-type (left) and *na2-1* seedlings (right) grown in the dark for 8 d. Red arrows indicate the distal end of the mesocotyls. D, Plant height of the wild type (WT) and *na2-1* measured from the soil line to the highest leaf collar. E, Internode lengths of the wild type and the *na2-1* mutant. Error bars are SD, and asterisks indicate Student's *t* test ($P < 0.01$) for comparisons between the wild type and *na2-1*. F to I, Photomicrographs of imprints from wild-type abaxial surface (F), *na2-1* abaxial surface (G), wild-type adaxial surface (H), or *na2-1* adaxial surface (I). Bars = 20 cm in A and B, 5 cm in C, and 50 μm in F to I.

and 16:15 [χ^2 P = 0.86], respectively; for data from complementation crosses, see Supplemental Table S1). The accessions in the stock center will retain the nomenclature they have carried to date, and line 4407D d*-N2374 was designated *na2-1*. The *na2-1* mutants were similar to *na1* in the effects on plant height, tiller formation repression, and the suppression of floral organ growth and development. The *na2-1* mutant was approximately 10% of the height of wild-type siblings at maturity and exhibited a tassel seed phenotype, displaying pistil development in the normally staminate tassel (Fig. 1, A, B, and D). The tassel seed phenotype of *na2-1* was not completely penetrant and was environmentally influenced. In the summer of 2014, 74 of 123 plants (60.2%) grown in the field exhibited some degree of tassel seed, whereas only three of 13 plants (23.1%) grown in the greenhouse exhibited tassel seed (Fisher's exact test P = 0.018). The *na2-1* mutant also showed a deetiolated phenotype when grown in the dark as compared with its wild-type siblings (Fig. 1C). Reduced height at maturity resulted from the compression of all internodes in *na2-1* as compared with wild-type siblings (Fig. 1, D and E). Stomatal imprints showed a slight difference in epidermal cell morphology between *na2* mutants and wild-type siblings (Fig. 1, F–I). No significant differences were identified in stomatal index or stomatal density for either the abaxial or adaxial surface of *na2-1* or *na2-2* mutants compared with wild-type siblings (Supplemental Table S2).

Due to the similarity in phenotypes of *na2* and *na1*, we measured endogenous BR intermediates to determine if the BR pathway was blocked. Table I summarizes the BR pathway intermediates measured in *na2-1* mutants and wild-type siblings. The *na2-1* mutants

Table I. *BR intermediates in wild-type and na2-1 plants*

Values shown are ng g^{-1} fresh weight from plants at 28 d after germination (DAG). Data are means of two independent experiments with 10 plants each. n.d., Not detected.

Compound	+/*na2-1*	*na2-1*/*na2-1*
24-Methylenecholesterol	1,950	12,550
Campesterol	21,650	167
Campestanol	442	3.62
6-Oxocampestanol	12.1	0.50
6-Deoxocathasterone	0.21	n.d.
6-Deoxoteasterone	0.04	n.d.
3-Dehydro-6-deoxoteasterone	0.41	n.d.
6-Deoxotyphasterol	2.71	n.d.
6-Deoxocastasterone	6.78	n.d.
Cathasterone	n.d.	n.d.
Teasterone	n.d.	n.d.
3-Dehydroteasterone	n.d.	n.d.
Typhasterol	0.04	n.d.
Castasterone	0.51	n.d.
Brassinolide	n.d.	n.d.

accumulated 6-fold greater levels of the BR intermediate 24-methylenecholesterol than wild-type plants. Consistent with a block in the BR pathway at this step, the level of the downstream intermediate campesterol was reduced by 130-fold in the mutant as compared with the wild type. The proposed pathway for BR biosynthesis in maize is presented in Supplemental Figure S1, and the block in campesterol production suggests that *na2* is defective in the C-24 reduction of 24-methylenechloesterol (Supplemental Fig. S1). This step in BR biosynthesis is encoded by the *DWARF1* (*DWF1*) gene in Arabidopsis (Choe et al., 1999).

The protein sequence encoded by *DWF1* was used as a query for a sequence similarity search by the BLAST algorithm (Tatusova and Madden, 1999) of the maize reference genome (AGPv3.21). This identified two predicted protein sequences in the maize genome as highly similar to DWF1 encoded by GRMZM2G057000 and GRMZM2G455658, both with greater than 79% identity to the DWF1 protein sequence. The conceptual translations of protein-coding sequences similar to DWF1 were obtained from whole-genome assemblies of plants available via Phytozome (Goodstein et al., 2012). A misannotation of the genes of maize, sorghum (*Sorghum bicolor*), and Selaginella (*Selaginella moellendorffii*) contains an N-terminal deletion, but closer inspection indicates conservation of these coding sequences within the regions annotated as 5′ untranslated region within GRZM2G455658, Sobic.004G355600, and Sm_144134, respectively. To investigate the phylogenetic relationships between the maize paralogs, *DWF1*, and the similar genes encoded in other plant genomes, we used a Bayesian Markov chain Monte Carlo approach implemented by MrBayes (Geyer, 1991; Ronquist et al., 2012) to construct the consensus tree depicted in Supplemental Figure S2. The tree is consistent with the two maize paralogs arising from a gene duplication that is older than the split between maize and sorghum. Analysis of the genomic contexts of both maize and sorghum genes using COGE GEVO (Lyons and Freeling, 2008) indicated extended regions of retained gene duplicates in comparisons between the sorghum paralogs, the maize paralogs, and the sorghum and maize paralog pairs. The extent of synteny was greater for paralogs that grouped together in the consensus tree (Supplemental Fig. S2; data not shown). Enzymes in this family are known to act on multiple substrates as Δ^{24}-sterol reductases (Klahre et al., 1998) and, thus, are not specific to BR biosynthesis. Consistent with their role in forming structural sterols, such as sitosterol, genes encoding presumptive 24-sterol reductase activity are widely phylogenetically distributed in plants. In agreement with previous studies, we identified similar sequences in both Physcomitrella (*Physcomitrella patens*) and Selaginella (Mizutani and Ohta, 2010; Cheon et al., 2013; Hamberger and Bak, 2013). Physcomitrella and Selaginella each encode two paralogs that derive from duplication after the divergence of those lineages from each other and the remainder of the taxa (Supplemental Fig. S2). Supplemental Figure S3 shows a multiple sequence alignment of the *na2* locus with Δ^{24}-sterol reductases from sorghum, *Setaria italica*, rice, Arabidopsis, *Glycine max*, *Manihot esculenta*, Selaginella, and Physcomitrella. Inspection of the two maize paralogs from the B73 reference genotype identified two frameshift mutations in GRMZM2G455658 that break and then restore the reading frame, resulting in more than 30 consecutive nonconserved amino acids disrupting a well-conserved region of the protein-coding sequence (Supplemental Fig. S3). Examination of the two sorghum paralogs also identified multiple frameshift mutations accumulated in the sorghum gene Sobic.004G355600 that disrupt extensive regions of conserved protein-coding sequences (Supplemental Fig. S3).

We determined the sequences of GRMZM2G057000 in multiple *na2* mutants. A summary of these data is presented in Figure 2, and the genetic material used is described in Supplemental Table S3. Sequencing of this locus in *na2-1* identified a C-to-T nucleotide transition at position 1,357 resulting in a premature stop codon and truncation of the last 110 amino acids (Fig. 2). Three additional alleles, *na2-2*, *na2-3*, and *na2-4*, were identified among plants with reduced stature in an ethyl methanesulfonate (EMS)-treated population derived from B73 (Weil, 2009). The *na2-2* mutant had a G-to-A transition at nucleotide position 658 resulting in a missense mutation that converted the Gly codon to Arg. Similarly, *na2-3* had a G-to-A transition at nucleotide position 463 resulting in a missense mutation that converted a Glu codon to Lys. These two missense mutations were drastic amino acid replacements that change codons that are 100% conserved between all angiosperms analyzed, as well as Selaginella and Physcomitrella, except for the missense mutation in *na2-2* in the sorghum paralog Sobic.004G355600 (Supplemental Fig. S3). The *na2-4* allele was a G-to-A

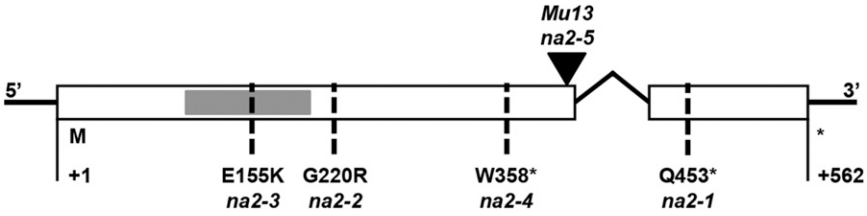

Figure 2. Structure of the *na2* locus and alleles. Exons are depicted as white boxes, the intron as a bent black line, and the sequence encoding the putative FAD-binding domain as a small gray box. Alleles are indicated with dashed lines for single-nucleotide polymorphism variations in *na2-1*, *na2-2*, *na2-3*, and *na2-4* and a triangle at the site of the *Mu13* transposable element insertion in *na2-5*. The amino acid substitution that results from each single-nucleotide polymorphism is specified above each allele designation, with an asterisk indicating the induction of a stop codon.

mutation at nucleotide position 1,074 resulting in a nonsense codon and truncation of the last 206 amino acids. We also generated an insertion allele, *na2-5*, in a targeted mutagenesis experiment among approximately 100,000 F1 plants from crosses using *na2-1* pollen onto *Mu*-active ears. The single novel allele, *na2-5*, contains a *Mu13* insertion at the codon for amino acid 407. Two additional alleles without molecular information were identified by allelism tests: *na2-6*, also taken from the maize B73 EMS population (Weil, 2009), and *na2-7*, which was in the 4405B d*-N1074C stock at the MaizeCOOP. All seven novel alleles of *na2* displayed similar dwarf phenotypes and rates of tassel seed production similar to the original mutant (Emerson et al., 1935).

NA2 mRNA Is Accumulated in Rapidly Growing Tissues of B73

We performed quantitative reverse transcription-PCR (qRT-PCR) to analyze the organ-specific expression of NA2. Figure 3 summarizes the means of relative expression normalized to controls for NA2 in mRNA extract from different organs and treatments of wild-type B73 plants. The NA2 transcript was detected in all tissues analyzed. The highest expression of NA2 was in mRNA from the collar (comprising the intercalary meristem, auricle, and ligule) of leaf 3 in plants at 9 DAG. The accumulation of NA2 was generally lower in older tissues. For example, the collar of leaf 13 taken from mature plants had less NA2 mRNA than the third leaf from 9-DAG plants. Interestingly, NA2 expression was low in the mesocotyl of dark-grown tissues despite the dependence of NA2 for elongation of this tissue, as indicated by the deetiolated phenotype of *na2-1* seedlings (Fig. 1C). Tissue age was not the only factor controlling NA2 expression. NA2 accumulation was strongly influenced by the linear axis of leaf expansion. The lowest NA2 mRNA expression was found in the blade of leaf 3 at 9 DAG, just distal to the collar that provided the highest observed NA2 accumulation.

Much like the frame-shift mutations that distinguished *na2* from *na2-like* (GRMZM2G455658; Supplemental Fig. S3), expression level differences between the paralogs also were visible. The accumulation of mRNA from *na2* was greater than that from the *na2-like* gene, as recorded in summaries of RNA sequencing experiments in the qTeller database (http://www.qteller.com). Shown in Supplemental Figure S4 are RNA fragments per kilobase of transcript per million mapped reads (FPKM) values for the two maize and two sorghum genes from the qTeller database. The maize *na2* gene (GRMZM2G057000) had an average FPKM value of 179.2 across all tissues and treatments, with the highest expression in the developing leaf (617; Supplemental Fig. S4A). The maize *na2-like* gene (GRMZM2G455658) had an average FPKM value of 0.1 across all tissues and treatments, with the highest expression in one of the pollen samples (2.9), but was inconsistently found in pollen RNA sequencing libraries (Supplemental Fig. S4B). The expression levels of the sorghum *na2* (Sobic.010G277300) and *na2-like* ortholog Sobic.004G355600 (Supplemental Fig. S2) had average FPKM values of 167.8 and 0.04, respectively (Supplemental Fig, S4, C and D). Thus, relative to their paralogs, the mRNA encoded by the *na2* genes was accumulated to 3 and 4 orders of magnitude greater levels and the *na2-like* paralogs had accumulated numerous frame-shift mutations after the divergence of maize and sorghum. This is consistent with the *na2-like* paralogs encoding pseudogenes that have lost expression and function. The observation that nonsense and missense mutations of GRMZM2G057000 were sufficient to dwarf maize plants favor this interpretation.

BR and GA Biosynthetic Mutants Exhibit Complex Genetic Interactions Controlling Organ Development and Growth

BR and GA biosynthetic mutants exhibit defects in floral development and severe dwarfism (Suttle, 1924; Hartwig et al., 2011). BR interacts with GA metabolism in rice (Schmitz et al., 2013; Tong et al., 2014) and at the signal transduction level in Arabidopsis (Bai et al., 2012; Li et al., 2012; Stewart Lilley et al., 2013). To investigate the BR and GA interaction in maize, we generated double mutants between BR and GA biosynthetic mutants. The BR mutants *na2-1* and *na1-1*, a 5α-steroid reductase, and the GA mutants *d1*, a GA

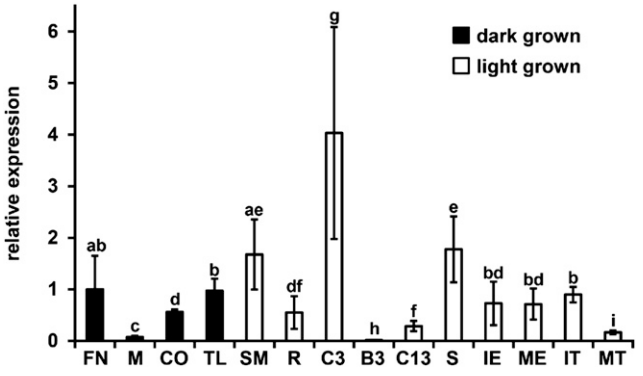

Figure 3. Comparison of relative NA2 mRNA accumulation measurement by qRT-PCR. qRT-PCR was carried out on mRNA extracted from multiple organs. Relative expression was obtained by normalization to the expression level of molybdenum cofactor (GRMZM2G067176) as an internal standard. Samples are indicated on the *x* axis: FN, 0.25-cm segment containing the first stem node of etiolated seedlings at 5 DAG; M, mesocotyl tissue of 5-DAG etiolated seedlings; CO, coleoptile of 5-DAG etiolated seedlings; TL, true leaves of 5-DAG etiolated seedlings; SM, shoot meristem and surrounding tissue of 9-DAG plants; R, roots of 9-DAG plants; C3, collar of the third leaf from 9-DAG plants; B3, blade from the third leaf of 9-DAG plants; C13, collar of the 13th leaf at maturity; S, stem segment from V7-stage plants; IE, immature ears 0.5 to 2.5 cm in length at the time of harvest; ME, mature ear sampled at silk emergence; IT, immature tassel 0.5 to 2.5 cm in length at the time of harvest; MT, mature tassel sampled at anthesis. Histogram height is proportional to the mean, and error bars indicate SD. Three biological replicates were run in three technical replications each for each sample. Lowercase letters indicate connecting letter report as determined by ANOVA with a posthoc analysis using the Holm-Sidak algorithm with $P < 0.05$. Samples that share the same letter do not differ statistically, whereas samples that are not connected by the same letter are statistically different.

3-oxidase, and *d5*, an *ent*-kaurene synthase, were used in this study (Hedden and Phinney, 1979; Hartwig et al., 2011; Chen et al., 2014). F2 populations from crosses between *na2-1* and *d5*, *na2-1* and *d1*, and *na1-1* and *d1* segregated for the mutants and effects of the genetic backgrounds. Some parental lines were of unknown backgrounds (Supplemental Table S3). To control for segregating background mutation effects, wild-type plants, single mutants, and double mutants were phenotyped and compared between F2 siblings to test BR and GA mutant effects without confounding the genetic background. The F2 generation of each cross was phenotyped for plant height, tiller number, anther ear formation, and production of tassel seeds in the summers of 2013 (*na2-1/d5*) and 2014 (*na2-1/d5*, *na2-1/d1*, and *na1-1/d1*). These results are summarized in Table II, and images of the resulting phenotypes are presented in Figure 4. Segregation ratios of phenotypes in the F2 generation were different from 9:3:3:1 for the *na2/d5* population (χ^2 $P = 5.43E\text{-}16$) and for the *na2-1/d1* population (χ^2 $P = 0.011$); however, the *na1-1/d1* population was not different from a 9:3:3:1 segregation (χ^2 $P = 0.400$). The *na2-1/d5* and *na2-1/d1* populations had an underrepresentation of single and double mutants as compared with wild-type plants. These results are consistent with weak seedling establishment in BR and GA mutants, as had been noted previously (Emerson et al., 1935).

The BR and GA biosynthetic mutations displayed multiple genetic interactions in the double mutants as compared with the single mutants. These interactions occurred in a development- and organ-specific manner. Wild-type plants on average were 180.2 cm, *na2-1* plants were 21.5 cm, *d5* plants were 30.3 cm, and *na2-1/d5* plants were 7.2 cm, with overall plant height being measured from the soil level to the leaf collar of the top leaf (Fig. 4, A–D; Table II). The *na2-1* and *d5* plants showed 88.1% and 83.2% reductions in plant height as compared with wild-type plants, respectively. The *na2-1/d5* double mutants were 96% reduced in plant height as compared with the wild type and 66.5% or 76.2% shorter than *na2-1* or *d5*, respectively. This demonstrates additivity and, thus, no interaction between *na2-1* and *d5* for overall plant height.

Unlike plant height, tillering displayed epistasis. A lack of endogenous GA causes maize plants to branch more and produce multiple tillers. By contrast, loss of BR biosynthesis suppressed tiller production. The *na2-1/d5* double mutants resembled the *na2-1* single mutants and did not display profuse tillers. The wild-type plants from the *na2-1* × *d5* F2 generation had 0.8 tillers per plant, no *na2-1* plants had tillers, *d5* mutants had an average of 2.1 tillers, and *na2-1 d5* had an average of 0.09 tillers, as only a single double mutant produced a single tiller (Fig. 4, A–D). These results demonstrate that *na2-1* is epistatic to *d5* for tiller production. This demonstrates that BR biosynthesis is required for a loss of GA to increase branch numbers.

BR and GA are required for the developmental failure of floral organs required to produce imperfect flowers in maize. BR mutants failed to suppress pistil development in the tassel, resulting in the tassel seed reported here (Fig. 1) and previously (Hartwig et al., 2011; Makarevitch et al., 2012). GA mutants failed to suppress anther development in the ear resulting in perfect flowers on the ear, also called anther ear (Emerson, 1912; Suttle, 1924; Evans and Poethig, 1995). To determine if these phenotypes were additive like plant height or displayed epistasis like tillering, the inflorescences of all F2 siblings in the cross between *na2-1* and *d5* were carefully observed for floral organ persistence. When tassel seeds were carefully phenotyped in the summers of 2013 and 2014 in the field, 0.3% (n = 658) of wild-type plants showed some degree of pistil production in the tassel. In the single mutants, 60% of *na2-1* plants (n = 123) and 0% of *d5* plants (n = 145) had tassel seeds. Double mutants were substantially suppressed as compared with *na2-1* single mutants, with 9% of *na2-1/d5* double mutant plants (n = 23) exhibiting some tassel seed formation (Fig. 4, E–H; Table II). This was greater than the wild type but far less than *na2-1* single mutants, suggesting that *d5* is required for the induction of tassel seeds mediated by the loss of *na2-1*.

Table II. *Morphometric analysis of BR and GA double mutant combinations*

Genotype	*n*	Height (cm)[a]	Tillers per Plant[a]	Plants with Tassel Seeds[b]	Plants with Anthers in Ear Florets[b]
na2-1 × *d5*; F2	949	–	–	–	–
Wild type	658	180.2 ± 21.2 a	0.8 ± 1.0 a	2 (0.3%) a	0 (0%) a
na2-1	123	21.5 ± 5.0 b	0 ± 0 b	74 (60%) b	0 (0%) a
d5	145	30.3 ± 5.7 c	2.1 ± 1.2 c	0 (0%) ac	145 (100%) b
na2-1/d5	23	7.2 ± 2.8 d	0.09 ± 0.3 d	2 (9%) c	22 (96%) b
na2-1 × *d1*; F2	576	–	–	–	–
Wild-type	349	193.9 ± 23.1 a	0.3 ± 0.6 a	3 (0.9%) a	0 (0%) a
na2-1	111	23.0 ± 6.1 b	0.0 ± 0.0 b	55 (50%) b	0 (0%) a
d1	97	37.6 ± 9.1 c	1.7 ± 1.2 c	0 (0%) a	97 (100%) b
na2-1/d1	19	7.3 ± 1.9 d	0.0 ± 0.0 d	1 (5%) a	19 (100%) b
na1-1 × *d1*; F2	172	–	–	–	–
Wild type	102	216.3 ± 22.9 a	0.7 ± 0.8 a	0 (0%) a	0 (0%) a
na1-1	35	51.7 ± 22.7 b	0.0 ± 0.0 b	6 (17%) b	0 (0%) a
d1	29	35.3 ± 7.8 c	2.0 ± 1.1 c	0 (0%) ab	29 (100%) b
na1-1/d1	6	14.2 ± 3.9 d	0.0 ± 0.0 d	0 (0%) ab	6 (100%) b

[a]Data are presented as means with SD. Lowercase letters indicate connecting letter report as determined by ANOVA with posthoc analysis using the Holm-Sidak algorithm with $P < 0.05$. [b]Number of plants with tassel seeds or anthers in ear florets, with the percentage of plants in parentheses. Lowercase letters indicate connecting letter report as determined by Fisher's exact test with $P < 0.01$.

The ears of the same plants were scored for anther production. Wild-type plants showed no development of anthers in ears (n = 658). The single mutants were differentially affected, with 0% of the *na2-1* plants displaying anther ear (n = 123) and 100% of *d5* plants developing anther ear (n = 145). Unlike tillering, where *na2-1* was epistatic to *d5*, 96% of *na2-1/d5* plants exhibited anther ear (n = 23; Fig. 4, I–L; Table II). This demonstrates that the persistence of anthers in the ears of *d5* mutants was not influenced by *na2-1* and the loss of BR.

The observations in all three double mutant combinations of the different BR and GA loci were mainly similar. The phenotyping results for all three F2 families can be found in Table II. The *na2-1/d1* double mutant combinations resulted in the same genetic interactions as described above for *na2-1/d5* double mutants. In addition, the phenotyping of the *na1-1/d1* double mutants showed identical genetic interactions between *na1-1* and *d1* as seen with *na2-1* and *d1* or *d5*. There were notable differences between the F2 populations, none of which altered the interaction between the BR and GA mutants. Most obvious among these are the increased height of *na1-1* single mutants and a lower percentage of tassel seed production (17%; n = 35) as compared with the *na2-1* mutants in

Table III. *Morphometric analysis of na2-1 treated with GA_3*

Parameter	Mock		+GA_3	
	+/na2-1	*na2-1/na2-1*	*+/na2-1*	*na2-1/na2-1*
n	16	13	16	14
Plant height[a]	192.9 ± 39.1 a	32.7 ± 5.7 b	309.6 ± 39.2 c	52.9 ± 16.8 d
Days to tassel[a]	63.8 ± 3.6 a	73.5 ± 8.6 b	60.0 ± 3.2 c	73.5 ± 5.3 b
Tillers per plant[a]	0 ± 0 a	0 ± 0 a	0 ± 0 a	0 ± 0 a
Plants with tassel seeds[b]	0 (0%) a	3 (23%) a,b	7 (44%) b	13 (93%) c
Plants with anthers in ear florets[b]	0 (0%) a	0 (0%) a	0 (0%) a	0 (0%) a
Tassel branches[a]	14.3 ± 5 a	11.7 ± 5.6 a	13.6 ± 4.2 a	11.9 ± 6.0 a
Total nodes[a]	15.1 ± 0.9 a	14.4 ± 1.3 a	15.5 ± 1.3 a	13.1 ± 1.1 b
Node of top ear[a]	10.4 ± 0.9 a	10.5 ± 1.1 a	9.9 ± 1.0 a,b	9.1 ± 1.0 b
Tassel length[a]	50.6 ± 4.2 a	28.2 ± 6.5 b	54.0 ± 13.5 a	31.7 ± 10.7 b
Angle of upper leaf[a]	25.9 ± 16.3 a	49.6 ± 19.9 b	23.8 ± 17.3 a	56.4 ± 17.7 b
Length of upper leaf[a]	48.8 ± 7.1 a,c	23.7 ± 8.5 b	42.0 ± 15.9 a	34.9 ± 10.1 c
Width of upper leaf[a]	5.4 ± 0.8 a	4.3 ± 1.0 b	3.5 ± 0.9 c	3.2 ± 0.9 c
Angle of lower leaf[a]	45.9 ± 14.7 a	61.2 ± 12.8 b	50.6 ± 9.8 a	74.5 ± 10.2 c
Length of lower leaf[a]	95.5 ± 9.6 a	61.4 ± 5.5 b	95.6 ± 14.8 a	77.8 ± 11.3 c
Width of lower leaf[a]	8.0 ± 0.9 a	8.1 ± 1.4 a	4.9 ± 1.2 b	4.3 ± 1.3 b

[a]Data are presented as means with SD. Lowercase letters indicate connecting letter report as determined by ANOVA with posthoc analysis using the Holm-Sidak algorithm with $P < 0.05$. [b]Number of plants with tassel seeds or anthers in ear florets, with the percentage of plants in parentheses. Lowercase letters indicate connecting letter report as determined by Fisher's exact test with $P < 0.01$.

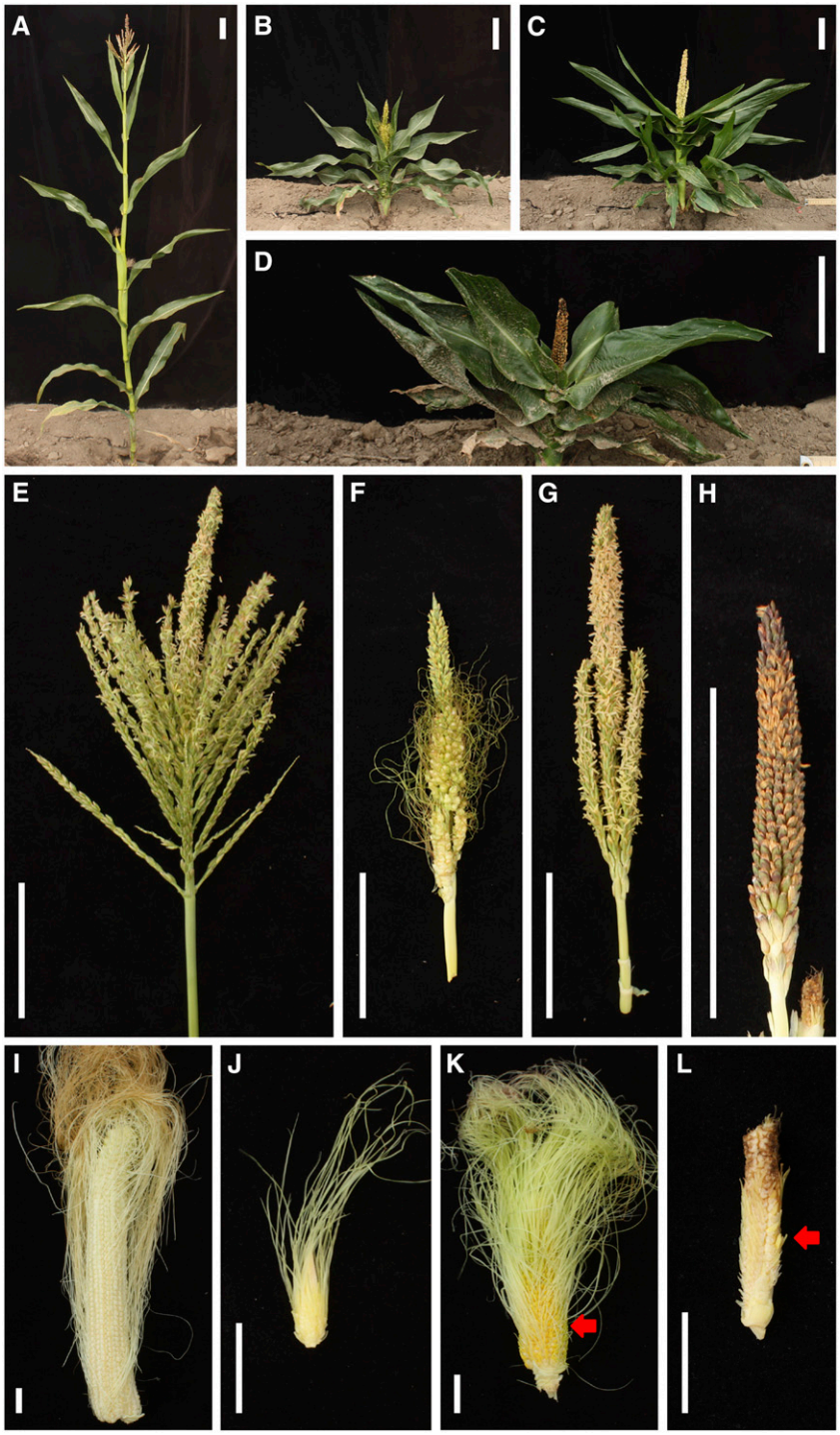

Figure 4. Morphological features of *na2-1*, *d5*, and double mutant combinations. All images were taken at maturity. A to D, Wild-type plant (A), *na2-1* plant (B), *d5* plant (C), and *na2-1/d5* plant (D). E to H, Tassel phenotypes of wild-type (E), *na2-1* (F), *d5* (G), and *na2-1/d5* (H) plants. I to L, Ear phenotypes of wild-type (I), *na2 -1* (J), *d5* (K), and *na2-1/d5* (L) plants. Silks have been partially removed from K and L. Red arrows indicate stamens on ears in K and L. Bars = 10 cm (A–H) and 2 cm (I–L).

the crosses to the same *d1* background. As a result of observing multiple phenotypes expressed in different developmental contexts, we find that there is no single mode of interaction between GA and BR in maize. In summary, BR and GA additively affected plant height, GA was required for the production of tassel seeds in the absence of BR, BR was required for the production of tillers in the absence of GA, but BR was not involved in the persistence of anthers in the ears that occurs in GA-deficient mutants.

Exogenous Application of *na2* and *d5* with GA_3

The double mutant analysis indicated multiple interactions between BR and GA affecting plant morphology. To investigate the effect of GA_3 on BR-dependent plant

architecture, *na2-1*, *d5*, and their wild-type siblings were treated with exogenous GA_3. GA_3 at 866 μM was applied directly into the leaf whorl as 1 mL every third day from 25 DAG until tassel emergence, similar to the approach taken by Nickerson (1959). Multiple phenotypes were measured, including plant height, tillers per plant, leaf angle, width and length of the leaf below the flag leaf and the leaf subtending the ear, node number, days to tassel, tassel branch number, tassel length, presence or absence of tassel seeds, and presence or absence of anthers in ear florets. The means and SD values of these measurements are presented in Table III. GA_3 application increased total plant height of both *na2-1* and the wild type (Table III). Plant height increased by similar amounts of 60% and 62% in wild-type and *na2-1* plants, respectively. This increase in height resulted in significant increases in all internodes except internode 14 of wild-type plants, whereas only internodes 1 to 4 and 7 were increased significantly in *na2-1* plants upon GA_3 application (Supplemental Fig. S5). These results are consistent with our observation of additivity between BR and GA disruption for plant height and indicate that BR-deficient mutants in maize respond to GA_3 treatment, resulting in internode elongation no different from that in the wild-type siblings.

Treatment with GA_3 caused the development of tassel seeds in wild-type plants and enhanced this phenotype in *na2-1* as compared with mock treatments (Table III). Thus, just as a loss of GA biosynthesis via the *d1* and *d5* mutants inhibited tassel seed production, exogenous GA_3 was sufficient to increase tassel seeds in both *na2-1* and the wild type. GA_3 application also accelerated tassel emergence in wild-type plants as compared with controls. This application had no effect on *na2-1* tassel emergence, indicating a BR dependence on GA_3-induced flowering time acceleration. The node carrying the top ear in *na2-1* plants was lower in GA_3-treated plants, which also produced fewer internodes overall. GA_3 treatment had no effect on internode number or ear placement, as detected in wild-type plants. This indicates that a loss of BR was necessary for GA_3 to influence internode number.

GA_3 caused *na2-1* upper (leaf below the top leaf) and lower (leaf above the node containing the uppermost ear) leaves to become narrower and longer. Wild-type leaf lengths were not affected by GA_3 treatment, but both upper and lower leaves were narrower (Table III). Applying GA_3 also resulted in an increase in the angle of the lower leaf for *na2-1* (more upright). Again, GA_3 treatment had no effect on leaf angles for wild-type plants. Thus, the loss of BR was required for this treatment to control leaf length and leaf angle. All other parameters measured showed no significant difference between GA_3 and mock treatment or *na2-1* and the wild type, respectively.

Some phenotypes were measured in these materials that had not been measured in our initial characterization of the *na2-1* mutant. Among these, significant differences were identified between *na2-1* and wild-type siblings. The angles of both the upper and lower leaves were significantly greater for *na2-1* plants as compared with wild-type plants in the untreated controls. In addition, the *na2-1* mutants exhibited shorter tassels than the wild-type plants under mock conditions. Although tassel branch numbers were lower in the *na2-1* mutants than in wild-type plants, the difference was not statistically significant, likely due to a remarkably high SD in tassel branch number in our conditions.

GA_3 effects on the single mutant *d5* also were scored, and means and SD values are summarized in Table IV. Applying GA_3 to *d5* and wild-type siblings resulted in a complementation of total plant height (Table IV). The GA_3 application increased all internode lengths in *d5* (Supplemental Fig. S5). The *d5* mutants took longer than the wild type to reach tassel emergence; however, GA_3 application resulted in *d5* reaching tassel emergence faster than mock treatment, although it did not completely recover delayed flowering time (Table IV). The excess tiller formation in *d5* mutants also was complemented by treatment with GA_3. Application of GA_3 resulted in the development of tassel seeds in 100% of *d5* plants, just as it had in wild-type plants (Table IV). This result provides a further test that the suppression of tassel seed production in the *na2-1*/*d5* double mutants was not due to a genetic background effect suppressing tassel seed formation. The GA_3 application failed to suppress the expression of anther ear in *d5* mutants, perhaps owing to the application to the whorl not delivering GA_3 to the ear branch at the time of floral organ specification and arrest. Tassel branches and tassel length were fewer and shorter, respectively, in *d5* compared with the wild type with mock treatment. Only tassel length was complemented in *d5* mutants upon GA_3 treatment, resulting in normal length tassels with fewer branches. The *d5* mutants had shorter and wider leaves as compared with the wild type under mock conditions. The leaf lengths were complemented upon GA_3 treatment, whereas *d5* leaves were narrower than both untreated *d5* and wild-type plants. In addition to the GA_3-affected phenotypes, the angle of the lower leaf of *d5* was significantly more upright than that of the wild type under control conditions and was unaffected by GA_3 treatment. All other parameters measured showed no significant difference between GA_3 and mock treatment or *d5* and wild-type contrasts.

DISCUSSION

We report here the molecular cloning of *na2*, the maize ortholog of the *DWF1* gene from Arabidopsis required for the conversion of 24-methylenecholesterol to campesterol in the BR biosynthesis pathway. The phenotype of *na2* was largely similar to the previously identified BR biosynthetic mutants of maize *na1* and *brd1* (Fig. 1; Hartwig et al., 2011; Makarevitch et al., 2012). BR intermediates were measured in the *na2-1* mutant and compared with controls (Table I). This identified a block in the conversion of 24-methylenecholesterol to campesterol

Table IV. *Morphometric analysis of d5 treated with GA_3*

Parameter	Mock		$+GA_3$	
	+/d5	*d5/d5*	*+/d5*	*d5/d5*
n	17	15	16	15
Plant height[a]	242.6 ± 28.9 a	38.8 ± 12.4 b	301.9 ± 40.9 c	313.3 ± 56.6 c
Days to tassel[a]	58.4 ± 3.6 a	71.7 ± 6.7 b	55.5 ± 6.9 a	61.6 ± 3.8 c
Tillers per plant[a]	0 ± 0 a	0.9 ± 0.9 b	0 ± 0 a,c	0.2 ± 0.4 c
Plants with tassel seeds[b]	0 (0%) a	0 (0%) a	16 (100%) b	15 (100%) b
Plants with anthers in ear florets[b]	0 (0%) a	15 (100%) b	0 (0%) a	15 (100%) b
Tassel branches[a]	21.8 ± 6.1 a	7.9 ± 5.7 b,c	16.3 ± 12.0 a,c	4.6 ± 3.2 b
Total nodes[a]	14.1 ± 1.1 a	14.5 ± 1.8 a	14.3 ± 1.1 a	13.5 ± 1.0 a
Node of top ear[a]	9.1 ± 0.6 a	8.7 ± 1.0 a	9.4 ± 0.7 a	9.1 ± 1.0 a
Tassel length[a]	61.2 ± 5.1 a	29.7 ± 3.5 b	56.3 ± 16.6 a,c	46.1 ± 11.9 c
Angle of upper leaf[a]	47.1 ± 17.1 a	47.0 ± 21.1 a	48.4 ± 13.1 a	50.7 ± 22.2 a
Length of upper leaf[a]	45.4 ± 5.5 a	28.4 ± 9.2 b	49.8 ± 10.8 a	50.3 ± 10.9 a
Width of upper leaf[a]	5.7 ± 0.6 a	7.3 ± 1.6 b	4.4 ± 1.6 c	3.6 ± 0.8 c
Angle of lower leaf[a]	47.9 ± 8.8 a	59.3 ± 11.6 b	47.8 ± 13.3 ab	55.7 ± 11.0 a,b
Length of lower leaf[a]	105.9 ± 7.6 a	50.7 ± 7.7 b	100.0 ± 10.3 a	92.5 ± 7.7 a
Width of lower leaf[a]	7.1 ± 0.7 a	9.6 ± 1.2 b	5.1 ± 1.2 a	3.8 ± 0.7 c

[a]Data are presented as means with SD. Lowercase letters indicate connecting letter report as determined by ANOVA with posthoc analysis using the Holm-Sidak algorithm with $P < 0.05$. [b]Number of plants with tassel seeds or anthers in ear florets, with the percentage of plants in parentheses. Lowercase letters indicate connecting letter report as determined by Fisher's exact test with $P < 0.01$.

in the mutant plants. Metabolite data served as an orthogonal data type that complemented a gene-based mapping and allele sequencing approach to confirm the *na2* gene identity as one of two *DWF1*-like sequences in maize. A total of seven alleles of *na2* were identified, five of which we also characterized molecularly with respect to the nature of the mutation (Fig. 2). All seven novel alleles of *na2* exhibited a phenotype comparable to the original *na2* allele identified by H.S. Perry in the 1930s (Emerson et al., 1935).

Many phenotypes observed in *na2* and other maize BR-deficient mutants indicated some lack of conservation for the effects of this phytohormone on plant development. The severe dwarfism of *na2* was similar to the effects of BR deficiency in other plants and resulted from a shortening of all internodes. The suppression of pistil development observed in maize has not been reported in the Arabidopsis mutants. Also in contrast to the Arabidopsis mutants, we found that the loss of BR biosynthesis downstream of *na2* was not required for stomata development in maize (Supplemental Table S2), unlike Arabidopsis, where BR affects the stomatal density and index (Gudesblat et al., 2012; Kim et al., 2012; Wang et al., 2015). This may be because BRs are not required for stomata production in all plants or may be due to an *na2*-independent production of bioactive BR in maize.

The persistence of pistils in the tassel of *na2* mutants required GA biosynthesis (Fig. 4; Table II). We also noted an environmental influence on this phenotype, with the expression of tassel seed production reduced in greenhouse conditions. Phenotype expression was strong in the winter nursery in PR (data not shown), indicating that it was not simply a daylength effect between our field and greenhouse experiments. Temperature, light quality and quantity, and rooting media influence all could be factors.

A phylogenetic analysis was performed using protein-coding sequences similar to Δ^{24}-sterol reductases from 36 plant taxa with fully sequenced genomes. This identified two paralogs each in maize and sorghum. These paralogs are the result of gene duplication prior to the divergence of maize and sorghum (Supplemental Fig. S2). Analysis of mRNA accumulation using the qTeller database found that mRNA from *na2* and the orthologous sorghum gene, Sobic.004G277300, were accumulated to at least 3 orders of magnitude greater counts than their paralogs, which showed very low or no detectable accumulation across all tissues and experiments (Supplemental Fig. S4). Analysis of the protein-coding sequences identified multiple frame-shift mutations that disrupted conserved regions of the maize (GRMZM2G455658) and sorghum (Sobic.004G355600) paralogs (Supplemental Fig. S3). These mutations were not shared between maize and sorghum but, rather, arose after the divergence of maize and sorghum. These frame-shift mutations resulted in poor multiple alignments (Supplemental Fig. S3). The presence of multiple independent frame-shift mutations that are likely to disrupt protein function and the observation of very low expression levels suggest that the *na2-like* subclade may have lost function already or be more prone to loss. In support of this possibility, this subclade is already absent in the genomes of *S. italica*, rice, and *Brachypodium distachyon*. It is also possible that the observed frame shifts resulted from poor genome assemblies. We were not able to test this with available EST sequences. The low expression level of the *na2-like* genes resulted in all EST data present in the National Center for Biotechnology Information being either derived from the *na2* orthologs or failing to cover the regions of the frame-shift mutations.

Interactions between BR and GA were demonstrated previously in Arabidopsis and rice (Bai et al., 2012; Li et al., 2012; Stewart Lilley et al., 2013; Tong et al., 2014). We have extended these observations of cross talk affecting plant development to maize. In addition, we have demonstrated many plant organs affected by the interaction between these phytohormones (Table II). The lack of a single conserved mode for the interaction demonstrates that plant height, tiller formation, and reproductive organ development will integrate the information from these two signals in some distinct manner and require the existence of a complex interaction scheme between BR- and GA-deficient mutants.

A model for the interactions between BR and GA that is consistent with our genetic interaction data is presented in Figure 5. Loss of *d5* or *d1* impacted apical dominance and increased tillering, which was suppressed by the loss of *na2* or *na1* (Table II). Thus, the tiller growth manifested in the absence of GA required BR production, and these experiments provide, to our knowledge, the first evidence in maize for BR tillering regulation. Tillering was shown previously to involve BR in other grasses such as barley (*Hordeum vulgare*) and rice (Tong et al., 2009; Hussien et al., 2014). Pistil production in the staminate tassel occurs in the *na2* and *na1* mutants, but mutation of *d5* or *d1* prevented tassel seed production (Fig. 4; Table II). This demonstrates that tassel seed production in the BR-deficient dwarves required GA. Furthermore, it suggested that the loss of BR results in tassel seed production by the overproduction of GA, similar to the tassel seed produced by sustained GA_3 applications performed by Nickerson (1959). GA production loss in the *d5* mutants resulted in anther ear development in maize, but unlike tillering, *na2* had no effect on this phenotype (Fig. 4; Table II). Thus, the interactions between BR and GA that result in their myriad effects on plant architecture were made up of a diverse set of interaction types. No developmental stage or organ type was predictive of the interaction. For example, the two phytohormones interacted to suppress pistils in the tassel but showed no interaction in stamen arrest in the ear florets, demonstrating that even for reproductive organ suppression, no one mode of interaction governed the outcome. By investigating other BR and GA biosynthetic mutant combinations and showing that the observed phenotypes are consistent with *na2*/*d5*, we demonstrate that they are not locus-specific interactions but reflect cross talk between BR and GA deficiency. Also, consistent with our observed dependence of tassel seed formation in *na2* and *na1* on GA biosynthesis (Table II), GA_3 application was able to induce tassel seed formation in *d5* and wild-type siblings (Table IV), indicating that excess GA in the tassel primordia was sufficient to block pistil abortion in the tassel florets even in the *d5* genetic background.

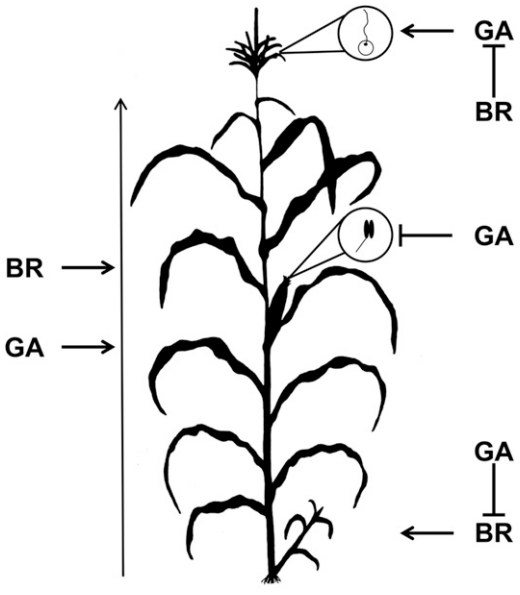

Figure 5. Model of the distinct interactions between *na2* and *d5* in different organs. BR and GA promote stem elongation and overall plant height additively. BR is required for the increase in tillering when GA is lost. GA suppresses anther formation in the ear independent of BR levels. GA is required for the production of pistil development in tassel florets when BR is absent. The vertical arrow at left of the maize plant indicates total plant height; lines with arrows represent positive regulation; lines with blocked arrows represent negative regulation.

GA_3 application to *na2-1* and *d5* allowed us to further elucidate the cross talk between BR and GA (Tables III and IV). GA_3 application results in fewer total nodes and a lower terminal ear node in *na2-1* but had no such effect on wild-type siblings. Thus, in the absence of BR, GA_3 application reduced node number. This reduction in node number was not associated with a decrease in flowering time. The *na2-1* mutants flowered later than the wild types in both mock and GA_3 treatments. GA_3 decreased flowering time for the wild type without changing node number (Table III). Thus, *na2-1* treated with GA_3 produced fewer nodes over a longer duration. This demonstrates a role for both BR and GA in determining the plastochron time, or time interval between each maize node initiation. The decrease in organ initiation rate by GA_3 in the *na2-1* plants is the opposite of what one would expect for GA, given the shorter flowering time in wild-type plants. This demonstrates that BR is required for GA to speed up flowering and increase the rate of new organ initiation. This is similar to the gating of GA effects by BR signaling in etiolating Arabidopsis hypocotyls (Bai et al., 2012). This may share a mechanistic relationship with tiller outgrowth, in which BR was required for the loss of GA to induce tiller outgrowth.

One maize BR-deficient phenotype demonstrated in this work is increased leaf angle, as reported previously of BR-deficient mutants in rice (Hong et al., 2004). Upright leaves are an agronomically important trait that contributed to increased planting densities and yield increases achieved by modern maize hybrids (Duvick, 2005). The *na2-1* mutants leaves were more upright than those of wild-type controls. Potentially contributing to this phenotype, the highest expression of NA2

was in young developing leaf collars (Fig. 3). NA2 mRNA accumulation also was relatively high in the shoot meristem and developing stem, with lower accumulation in the leaf blade (Fig. 3). The abundant expression of this gene raises the possibility that manipulation of BR levels can be used for crop improvement. We demonstrated that we can simultaneously reduce plant height and increase leaf angle. This could both improve harvest index and allow for greater maize planting densities. GA_3 treatment to *na2-1* plants resulted in further increases to leaf angles (Table III). Thus, BR reduction sensitized the leaf collar to GA_3 treatment. In contrast, it was shown in rice that GA inhibited lamina inclination with accumulated BR or enhanced BR signaling (Tong et al., 2014). Leaf length also was strongly dependent on BR and GA, but in this case, GA only increased leaf length in the absence of BR. This should be interpreted with caution, however, as treatment with GA_3 was performed by application into the whorl, which may deliver GA_3 to the site of leaf primordia initiation, young leaves during expansion, and meristems but not over the entire developmental phase of the leaf or post intercalary meristem expansion of the blade. The observations of elongated leaves in *na2-1* suggest that defects in growth established early in leaf development by a loss of BR can be partially overcome by GA_3 applications.

MATERIALS AND METHODS

Plant Material and Growth Conditions

All of the maize (*Zea mays*) genetic stocks used in this study are summarized in Supplemental Table S3. The *na2-506D* and *na2-518C* stocks were obtained from the MaizeCOOP as lines 506D and 518C, respectively. The *na2-1* and *na2-7* alleles were obtained from the MaizeCOOP as lines 4407D d*-N2374 and 4405B d*-N1074C, respectively. *na2-2* (PB03NM417), *na2-3* (04INW22CW04351), *na2-4* (04IAB73PS020G1), and *na2-6* (04CAB73SH0365) were identified in an EMS population as M3 generation plants in the summer of 2011. *na2-5* was identified as an F1 plant in a *Mu*-tagging screen of approximately 120,000 plants crossed with *na2-1* in the summer of 2012. Seeds of the *d5* mutant were obtained from the Carolina Biological Supply Company as item 177110. The *d1* allele used was obtained from the MaizeCOOP as line 302A *d1*-6016. The *na1-1* allele (Hartwig et al., 2011) corresponds to line 310G in the Maize COOP. The GRMZM2G057000 locus was amplified from the *na2-1* to *na2-5* alleles using primers described in Supplemental Table S4. PCR products were sequenced using the Sanger method (Sanger et al., 1977; Macrogen USA).

Double mutant analyses were conducted on plants grown in the field in West Lafayette, Indiana, at the Agronomy Center for Research and Education in the summer of 2013 (*na2*/*d5*) and 2014 (*na2*/*d5*, *na2*/*d1*, and *na1*/*d1*). All greenhouse experiments were conducted in the Purdue Horticulture Plant Growth Facility using temperature settings of 27°C (day) and 21°C (night) with a 16-h daylength provided by supplemental lighting, as needed. Plants were fertilized with 200 ppm Miracle-Gro Excel (Scotts) adjusted to pH 6 following the manufacturer's recommendations.

The plant tissue used for qRT-PCR analysis of gene expression in dark-grown material was collected from 5-DAG etiolated plants of B73 grown in type 601 flat trays filled with Turface MVP (Profile Products) as the potting substrate. Plants were grown in complete darkness in a Conviron E8 growth chamber at 27°C. The material sampled included a 0.25-cm segment containing the first stem node, mesocotyl tissue, coleoptile tissue, and the true leaves. Light-grown tissues for qRT-PCR analysis of gene expression were sampled from 9-DAG seedlings in Turface incubated in the greenhouse conditions described above. Material collected included the shoot meristem and surrounding tissue, roots, the leaf collar of the third leaf, and the third leaf blade cut through the intercalary meristem. Nonseedling tissues collected from light-grown plants were collected from plants grown in the field. These included the uppermost stem segments from V7-stage plants that were 1 cm in length, immature ears 0.5 to 2.5 cm in length at the time of harvest, mature ears collected at silk emergence from the husks, immature tassels 0.5 to 2.5 cm in length at the time of harvest, and mature tassels harvested at anthesis.

Leaf Imprints for Microscopic Analysis of Stomata Development

Wild-type, *na2-1*, and *na2-2* families were grown for 28 DAG (V5 stage) in the greenhouse under the conditions stated previously. Epidermal cell layer imprints were produced from the widest portion of the fifth leaf using ethyl 2-cyanoacrylate (Scotch SuperGlue; 3M) applied to the leaves and then pressed onto and recovered on glass microscope slides (Thermo Fisher Scientific). Imprints of the adaxial and abaxial leaf surfaces were taken and observed by light microscopy using a UNICO H606T microscope (United Products & Instruments). Stomatal indices and densities were calculated for each imprint by counting all the cells in five randomly selected viewable areas in each imprint at 40× magnification. Only areas between vasculature tissues from high-quality imprints where all cell boundaries were completely visible were considered. For each genotype, mean parameters were calculated from five viewable areas from each of six plants per genotype.

Quantification of BR Intermediates

For internal BR measurements, wild-type and *na2-1* siblings were grown for 28 d in the greenhouse, and shoot tissue was harvested and immediately frozen in liquid nitrogen. Samples were then lyophilized using the VirTis 2KBTES-55 freeze dryer (SP Scientific) for 3 d at −78°C and 0.53 Pa. Purification and quantification of BR was performed as described (Fujioka et al., 2002). A summary of the two independent experiments is shown in Supplemental Table S5.

Phylogenetic Analyses and in Silico Analysis of Expression Data

GRMZM2G057000 protein homolog DNA-coding sequences were obtained using the Inparanoid method (O'Brien et al., 2005) through Phytozome version 10.2.2 (Goodstein et al., 2012) with a Dual Affine Smith-Waterman alignment score greater than 1,500, and a sequence similarity of greater than 50% resulted in a total of 57 sequences from 36 taxa. All sequences were downloaded using BioMart (Smedley et al., 2015) and loaded into Mesquite version 3.03 (Maddison and Maddison, 2015), where they were aligned using ClustalW version 2.1 (Larkin et al., 2007). FastTree version 2.1.7 (Price et al., 2010) was used to create an approximate maximum-likelihood phylogenetic tree from the aligned sequences. The maximum-likelihood tree was used as a starting tree for MrBayes version 3.2.5 (Ronquist et al., 2012) to infer a Markov chain Monte Carlo (Geyer, 1991) phylogenetic tree using a general time reversible model with a proportion of invariable sites and a γ-shaped distribution of rates across sites model with a variable partition rate (rates varied under a flat Dirichlet prior). The analysis was run for 10 million generations.

FPKM values and histograms were obtained from qteller.com for selected maize and sorghum (*Sorghum bicolor*) genes (Wang et al., 2009; Li et al., 2010; Davidson et al., 2011, 2012; Dugas et al., 2011; Schnable and Freeling, 2011; Waters et al., 2011; Bolduc et al., 2012; Chang et al., 2012; Kakumanu et al., 2012; Mizuno et al., 2012). Recreation of these histograms could be obtained at http://www.qteller.com.

qRT-PCR

Total RNA was isolated as described (Sekhon et al., 2011) from various B73 tissues and treated with DNaseI (Thermo Fisher Scientific). Complementary DNA was synthesized using reverse transcriptase (iScript; Bio-Rad) according to the manufacturer's instructions. All primers used for qRT-PCR analysis are described in Supplemental Table S4 and were designed using PrimerExpress software (Applied Biosystems, Invitrogen). All primers used showed 90% to 110% efficiency at 500 nM concentration when conducting complementary DNA dilution standard curves using StepOne software (Applied Biosystems, Invitrogen) for amplification efficiency (Taylor et al., 2010). The molybdenum cofactor biosynthesis gene (GRMZM2G067176) was used as the internal control

(Sekhon et al., 2011). The StepOnePlus (Applied Biosystems, Invitrogen) instrument was used as described (Orlova et al., 2009) to conduct qRT-PCR.

GA_3 Experiments

Maize plants treated with GA_3 were grown under greenhouse conditions as stated previously. Plants were grown in 2-gallon pots with a 2:1 mixture of Turface MVP (Profile Products) to peat germinating mix (Conrad Fafard). GA_3 (Gold Biotechnology) at 866 μM in water with a final concentration of 0.02% ethanol and 0.005% Silwet L-77 (Sigma-Aldrich) or a mock preparation of ethanol and Silwet L-77 without GA was applied to the leaf whorl every third day, starting 25 d after planting until tassel emergence. All measurements were taken at maturity.

Statistical Analyses

Microsoft Excel and the add-in XL Toolbox (version 6.50; http://xltoolbox.sourceforge.net) was used for statistical analysis. ANOVA for sets of data groups was performed with multiple comparisons/post hoc testing within XL Toolbox. If a significant difference ($P < 0.05$) was detected, post hoc tests using a Holm-Sidak correction for multiple tests (Zar, 2010) were performed. The Microsoft Excel add-in Real Statistics Resource Pack (version 3.3.1; http://real-statistics.com) was used for hypothesis testing on binary data. The Real Statistics Resource Pack formula for Fisher's exact test was used to determine significant differences ($P < 0.01$) between samples, and then multiple comparisons were conducted between data groups (Zar, 2010).

Accession Numbers

Sequence data from this article can be found in the GenBank/EMBL data libraries under the following accession numbers: KX443688 (*na2-1*), KX443689 (*na2-2*), KX443690 (*na2-3*), KX443691 (*na2-4*), and KX443692 (*na2-5*).

Supplemental Data

The following supplemental materials are available.

Supplemental Figure S1. Proposed BR pathway and measured intermediates from *na2-1* and wild-type plants.

Supplemental Figure S2. Phylogenetic tree of presumed Δ^{24}-sterol reductases from 36 taxa.

Supplemental Figure S3. Multiple sequence alignment of maize NA2 protein sequence with orthologous sequences.

Supplemental Figure S4. RNA expression levels of maize or sorghum genes from the qTeller data set.

Supplemental Figure S5. Internode lengths of *na2-1*, *d5*, and wild-type siblings with and without GA_3 application.

Supplemental Table S1. Segregation ratios of crosses.

Supplemental Table S2. Stomatal indices and densities of *na2-1*, *na2-2*, and wild-type plants.

Supplemental Table S3. Sources of maize genetic stocks.

Supplemental Table S4. Primers used in this study.

Supplemental Table S5. Two independent experiments showing BR intermediates in wild-type and *na2-1* plants.

ACKNOWLEDGMENTS

We thank Jim Beaty and the Purdue University Agronomy Farm for expert assistance as well as Rob Eddy and the greenhouse team for the Horticulture Greenhouse facility for the production of high-quality growth environments; Johal laboratory members A. DeLeon, R. Zhan, and K. Chu for help with chemical treatments; and Dilkes laboratory members E. Buescher, C. Addo-Quaye, and M. Silva Guzman for reading early drafts of the article and returning comments.

Received March 10, 2016; accepted May 15, 2016; published June 10, 2016.

LITERATURE CITED

Acosta IF, Laparra H, Romero SP, Schmelz E, Hamberg M, Mottinger JP, Moreno MA, Dellaporta SL (2009) *tasselseed1* is a lipoxygenase affecting jasmonic acid signaling in sex determination of maize. Science **323:** 262–265

Bai MY, Shang JX, Oh E, Fan M, Bai Y, Zentella R, Sun TP, Wang ZY (2012) Brassinosteroid, gibberellin and phytochrome impinge on a common transcription module in Arabidopsis. Nat Cell Biol **14:** 810–817

Bolduc N, Yilmaz A, Mejia-Guerra MK, Morohashi K, O'Connor D, Grotewold E, Hake S (2012) Unraveling the KNOTTED1 regulatory network in maize meristems. Genes Dev **26:** 1685–1690

Chang YM, Liu WY, Shih AC, Shen MN, Lu CH, Lu MY, Yang HW, Wang TY, Chen SC, Chen SM, et al (2012) Characterizing regulatory and functional differentiation between maize mesophyll and bundle sheath cells by transcriptomic analysis. Plant Physiol **160:** 165–177

Chapin FS, Bloom AJ, Field CB, Waring RH (1987) Plant responses to multiple environmental factors. Bioscience **37:** 49–57

Chen Y, Hou M, Liu L, Wu S, Shen Y, Ishiyama K, Kobayashi M, McCarty DR, Tan BC (2014) The maize DWARF1 encodes a gibberellin 3-oxidase and is dual localized to the nucleus and cytosol. Plant Physiol **166:** 2028–2039

Cheon J, Fujioka S, Dilkes BP, Choe S (2013) Brassinosteroids regulate plant growth through distinct signaling pathways in Selaginella and Arabidopsis. PLoS ONE **8:** e81938

Choe S, Dilkes BP, Gregory BD, Ross AS, Yuan H, Noguchi T, Fujioka S, Takatsuto S, Tanaka A, Yoshida S, et al (1999) The Arabidopsis *dwarf1* mutant is defective in the conversion of 24-methylenecholesterol to campesterol in brassinosteroid biosynthesis. Plant Physiol **119:** 897–907

Choe S, Fujioka S, Noguchi T, Takatsuto S, Yoshida S, Feldmann KA (2001) Overexpression of DWARF4 in the brassinosteroid biosynthetic pathway results in increased vegetative growth and seed yield in Arabidopsis. Plant J **26:** 573–582

Chuck G, Meeley R, Irish E, Sakai H, Hake S (2007) The maize *tasselseed4* microRNA controls sex determination and meristem cell fate by targeting *tasselseed6/indeterminate spikelet1*. Nat Genet **39:** 1517–1521

Davidson RM, Gowda M, Moghe G, Lin H, Vaillancourt B, Shiu SH, Jiang N, Buell CR (2012) Comparative transcriptomics of three Poaceae species reveals patterns of gene expression evolution. Plant J **71:** 492–502

Davidson RM, Hansey CN, Gowda M, Childs KL, Lin H, Vaillancourt B, Sekhon RS, de Leon N, Kaeppler SM, Jiang N, et al (2011) Utility of RNA sequencing for analysis of maize reproductive transcriptomes. Plant Genome **4:** 191–203

DeLong A, Calderon-Urrea A, Dellaporta SL (1993) Sex determination gene TASSELSEED2 of maize encodes a short-chain alcohol dehydrogenase required for stage-specific floral organ abortion. Cell **74:** 757–768

Depuydt S, Hardtke CS (2011) Hormone signalling crosstalk in plant growth regulation. Curr Biol **21:** R365–R373

Dugas DV, Monaco MK, Olsen A, Klein RR, Kumari S, Ware D, Klein PE (2011) Functional annotation of the transcriptome of *Sorghum bicolor* in response to osmotic stress and abscisic acid. BMC Genomics **12:** 514

Duvick DN (2005) The contribution of breeding to yield advances in maize (*Zea mays* L.). Adv Agron **86:** 83–145

Eckardt NA (2002) Foolish seedlings and DELLA regulators: the functions of rice SLR1 and *Arabidopsis* RGL1 in GA signal transduction. Plant Cell **14:** 1–5

Elfving DC, Visser DB, Henry JL (2011) Gibberellins stimulate lateral branch development in young sweet cherry trees in the orchard. Int J Fruit Sci **11:** 41–54

Emerson RA (1912) The inheritance of certain "abnormalities" in maize. Am Breeders Assoc Annu Rep **7/8:** 385–399

Emerson RA, Beadle GW, Fraser AC (1935) A summary of linkage studies in maize. Cornell Univ Agric Exp Stn Mem 1–83

Evans MM, Poethig RS (1995) Gibberellins promote vegetative phase change and reproductive maturity in maize. Plant Physiol **108:** 475–487

Fujioka S, Takatsuto S, Yoshida S (2002) An early C-22 oxidation branch in the brassinosteroid biosynthetic pathway. Plant Physiol **130:** 930–939

Geyer CJ (1991) Markov chain Monte Carlo maximum likelihood. *In* M Keramidas, ed, Computing Science and Statistics: Proceedings of the 23rd Symposium on the Interface. Interface Foundation of North America, Fairfax Station, VA, pp 156–163

Goodstein DM, Shu S, Howson R, Neupane R, Hayes RD, Fazo J, Mitros T, Dirks W, Hellsten U, Putnam N, et al (2012) Phytozome: a comparative platform for green plant genomics. Nucleic Acids Res **40:** D1178–D1186

Gudesblat GE, Schneider-Pizoń J, Betti C, Mayerhofer J, Vanhoutte I, van Dongen W, Boeren S, Zhiponova M, de Vries S, Jonak C, et al (2012) SPEECHLESS integrates brassinosteroid and stomata signalling pathways. Nat Cell Biol **14:** 548–554

Hamant O, Traas J (2010) The mechanics behind plant development. New Phytol **185:** 369–385

Hamberger B, Bak S (2013) Plant P450s as versatile drivers for evolution of species-specific chemical diversity. Philos Trans R Soc Lond B Biol Sci **368:** 20120426

Hartwig T, Chuck GS, Fujioka S, Klempien A, Weizbauer R, Potluri DPV, Choe S, Johal GS, Schulz B (2011) Brassinosteroid control of sex determination in maize. Proc Natl Acad Sci USA **108:** 19814–19819

Hedden P, Phinney BO (1979) Comparison of ent-kaurene and ent-isokaurene synthesis in cell-free systems from etiolated shoots of normal and dwarf-5 maize seedlings. Phytochemistry **18:** 1475–1479

Hong Z, Ueguchi-Tanaka M, Matsuoka M (2004) Brassinosteroids and rice architecture. J Pestic Sci **29:** 184–188

Hussien A, Tavakol E, Horner DS, Muñoz-Amatriaín M, Muehlbauer GJ, Rossini L (2014) Genetics of tillering in rice and barley. Plant Genome **7:** 1–20

Irish EE, Langdale JA, Nelson TM (1994) Interactions between tassel seed genes and other sex-determining genes in maize. Dev Genet **15:** 155–171

Jaillais Y, Chory J (2010) Unraveling the paradoxes of plant hormone signaling integration. Nat Struct Mol Biol **17:** 642–645

Kakumanu A, Ambavaram MM, Klumas C, Krishnan A, Batlang U, Myers E, Grene R, Pereira A (2012) Effects of drought on gene expression in maize reproductive and leaf meristem tissue revealed by RNA-Seq. Plant Physiol **160:** 846–867

Kim B, Kwon M, Jeon J, Schulz B, Corvalán C, Jeong YJ, Choe S (2014) The Arabidopsis *gulliver2/phyB* mutant exhibits reduced sensitivity to brassinazole. J Plant Biol **57:** 20–27

Kim TW, Michniewicz M, Bergmann DC, Wang ZY (2012) Brassinosteroid regulates stomatal development by GSK3-mediated inhibition of a MAPK pathway. Nature **482:** 419–422

Klahre U, Noguchi T, Fujioka S, Takatsuto S, Yokota T, Nomura T, Yoshida S, Chua NH (1998) The *Arabidopsis DIMINUTO/DWARF1* gene encodes a protein involved in steroid synthesis. Plant Cell **10:** 1677–1690

Larkin MA, Blackshields G, Brown NP, Chenna R, McGettigan PA, McWilliam H, Valentin F, Wallace IM, Wilm A, Lopez R, et al (2007) Clustal W and Clustal X version 2.0. Bioinformatics **23:** 2947–2948

Li L, Xu J, Xu ZH, Xue HW (2005) Brassinosteroids stimulate plant tropisms through modulation of polar auxin transport in Brassica and *Arabidopsis*. Plant Cell **17:** 2738–2753

Li P, Ponnala L, Gandotra N, Wang L, Si Y, Tausta SL, Kebrom TH, Provart N, Patel R, Myers CR, et al (2010) The developmental dynamics of the maize leaf transcriptome. Nat Genet **42:** 1060–1067

Li QF, Wang C, Jiang L, Li S, Sun SSM, He JX (2012) An interaction between BZR1 and DELLAs mediates direct signaling crosstalk between brassinosteroids and gibberellins in Arabidopsis. Sci Signal **5:** ra72–ra72

Lyons E, Freeling M (2008) How to usefully compare homologous plant genes and chromosomes as DNA sequences. Plant J **53:** 661–673

Maddison WP, Maddison DR (2015) Mesquite: a modular system for evolutionary analysis, version 3.03. http://mesquiteproject.org

Makarevitch I, Thompson A, Muehlbauer GJ, Springer NM (2012) *Brd1* gene in maize encodes a brassinosteroid C-6 oxidase. PLoS ONE **7:** e30798

Mizuno H, Kawahigashi H, Kawahara Y, Kanamori H, Ogata J, Minami H, Itoh T, Matsumoto T (2012) Global transcriptome analysis reveals distinct expression among duplicated genes during sorghum-*Bipolaris sorghicola* interaction. BMC Plant Biol **12:** 121

Mizutani M, Ohta D (2010) Diversification of P450 genes during land plant evolution. Annu Rev Plant Biol **61:** 291–315

Nakashita H, Yasuda M, Nitta T, Asami T, Fujioka S, Arai Y, Sekimata K, Takatsuto S, Yamaguchi I, Yoshida S (2003) Brassinosteroid functions in a broad range of disease resistance in tobacco and rice. Plant J **33:** 887–898

Nemhauser JL, Hong F, Chory J (2006) Different plant hormones regulate similar processes through largely nonoverlapping transcriptional responses. Cell **126:** 467–475

Nickerson NH (1959) Sustained treatment with gibberellic acid of five different kinds of maize. Ann Mo Bot Gard **46:** 19–37

O'Brien KP, Remm M, Sonnhammer EL (2005) Inparanoid: a comprehensive database of eukaryotic orthologs. Nucleic Acids Res **33:** D476–D480

Oh E, Zhu JY, Bai MY, Arenhart RA, Sun Y, Wang ZY (2014) Cell elongation is regulated through a central circuit of interacting transcription factors in the Arabidopsis hypocotyl. eLife **3:** 1–19

Oh E, Zhu JY, Wang ZY (2012) Interaction between BZR1 and PIF4 integrates brassinosteroid and environmental responses. Nat Cell Biol **14:** 802–809

Orlova I, Nagegowda DA, Kish CM, Gutensohn M, Maeda H, Varbanova M, Fridman E, Yamaguchi S, Hanada A, Kamiya Y, et al (2009) The small subunit of snapdragon geranyl diphosphate synthase modifies the chain length specificity of tobacco geranylgeranyl diphosphate synthase in planta. Plant Cell **21:** 4002–4017

Orshan G (1986) Plant form as describing vegetation and expressing adaptation to environment. Ann Bot (Lond) **44:** 7–38

Price MN, Dehal PS, Arkin AP (2010) FastTree 2: approximately maximum-likelihood trees for large alignments. PLoS ONE **5:** e9490

Ronquist F, Teslenko M, van der Mark P, Ayres DL, Darling A, Höhna S, Larget B, Liu L, Suchard MA, Huelsenbeck JP (2012) MrBayes 3.2: efficient Bayesian phylogenetic inference and model choice across a large model space. Syst Biol **61:** 539–542

Saibo NJ, Vriezen WH, Beemster GT, Van Der Straeten D (2003) Growth and stomata development of Arabidopsis hypocotyls are controlled by gibberellins and modulated by ethylene and auxins. Plant J **33:** 989–1000

Sakamoto T, Morinaka Y, Ohnishi T, Sunohara H, Fujioka S, Ueguchi-Tanaka M, Mizutani M, Sakata K, Takatsuto S, Yoshida S, et al (2006) Erect leaves caused by brassinosteroid deficiency increase biomass production and grain yield in rice. Nat Biotechnol **24:** 105–109

Salamini F (2003) Hormones and the green revolution. Science **302:** 71–72

Salas Fernandez MG, Becraft PW, Yin Y, Lübberstedt T (2009) From dwarves to giants? Plant height manipulation for biomass yield. Trends Plant Sci **14:** 454–461

Sanger F, Nicklen S, Coulson AR (1977) DNA sequencing with chain-terminating inhibitors. Proc Natl Acad Sci USA **74:** 5463–5467

Santner A, Calderon-Villalobos LI, Estelle M (2009) Plant hormones are versatile chemical regulators of plant growth. Nat Chem Biol **5:** 301–307

Santner A, Estelle M (2009) Recent advances and emerging trends in plant hormone signalling. Nature **459:** 1071–1078

Schmitz AJ, Folsom JJ, Jikamaru Y, Ronald P, Walia H (2013) SUB1A-mediated submergence tolerance response in rice involves differential regulation of the brassinosteroid pathway. New Phytol **198:** 1060–1070

Schnable JC, Freeling M (2011) Genes identified by visible mutant phenotypes show increased bias toward one of two subgenomes of maize. PLoS ONE **6:** e17855

Sekhon RS, Lin H, Childs KL, Hansey CN, Buell CR, de Leon N, Kaeppler SM (2011) Genome-wide atlas of transcription during maize development. Plant J **66:** 553–563

Smedley D, Haider S, Durinck S, Pandini L, Provero P, Allen J, Arnaiz O, Awedh MH, Baldock R, Barbiera G, et al (2015) The BioMart community portal: an innovative alternative to large, centralized data repositories. Nucleic Acids Res **43:** W589–W598

Stewart Lilley JL, Gan Y, Graham IA, Nemhauser JL (2013) The effects of DELLAs on growth change with developmental stage and brassinosteroid levels. Plant J **76:** 165–173

Sussex IM, Kerk NM (2001) The evolution of plant architecture. Curr Opin Plant Biol **4:** 33–37

Suttle A (1924) The genetic interrelations of different types of dwarf corn. PhD thesis. Cornell University, Ithaca, NY

Tatusova TA, Madden TL (1999) BLAST 2 Sequences, a new tool for comparing protein and nucleotide sequences. FEMS Microbiol Lett **174:** 247–250

Taylor S, Wakem M, Dijkman G, Alsarraj M, Nguyen M (2010) A practical approach to RT-qPCR-Publishing data that conform to the MIQE guidelines. Methods **50:** S1–S5

Tong H, Jin Y, Liu W, Li F, Fang J, Yin Y, Qian Q, Zhu L, Chu C (2009) DWARF AND LOW-TILLERING, a new member of the GRAS family, plays positive roles in brassinosteroid signaling in rice. Plant J **58:** 803–816

Tong H, Xiao Y, Liu D, Gao S, Liu L, Yin Y, Jin Y, Qian Q, Chu C (2014) Brassinosteroid regulates cell elongation by modulating gibberellin metabolism in rice. Plant Cell **26:** 4376–4393

Vanstraelen M, Benková E (2012) Hormonal interactions in the regulation of plant development. Annu Rev Cell Dev Biol **28:** 463–487

Vert G, Walcher CL, Chory J, Nemhauser JL (2008) Integration of auxin and brassinosteroid pathways by Auxin Response Factor 2. Proc Natl Acad Sci USA **105:** 9829–9834

Wada K, Marumo S, Ikekawa N, Morisaki M, Mori K (1981) Brassinolide and homobrassinolide promotion of lamina inclination of rice seedlings. Plant Cell Physiol **2:** 323–325

Wang M, Yang K, Le J (2015) Organ-specific effects of brassinosteroids on stomatal production coordinate with the action of *Too Many Mouths*. J Integr Plant Biol **57:** 247–255

Wang X, Elling AA, Li X, Li N, Peng Z, He G, Sun H, Qi Y, Liu XS, Deng XW (2009) Genome-wide and organ-specific landscapes of epigenetic modifications and their relationships to mRNA and small RNA transcriptomes in maize. Plant Cell **21:** 1053–1069

Wang Y, Li L, Ye T, Zhao S, Liu Z, Feng YQ, Wu Y (2011) Cytokinin antagonizes ABA suppression to seed germination of Arabidopsis by downregulating ABI5 expression. Plant J **68:** 249–261

Wang Y, Sun S, Zhu W, Jia K, Yang H, Wang X (2013) Strigolactone/MAX2-induced degradation of brassinosteroid transcriptional effector BES1 regulates shoot branching. Dev Cell **27:** 681–688

Waters AJ, Makarevitch I, Eichten SR, Swanson-Wagner RA, Yeh CT, Xu W, Schnable PS, Vaughn MW, Gehring M, Springer NM (2011) Parent-of-origin effects on gene expression and DNA methylation in the maize endosperm. Plant Cell **23:** 4221–4233

Weil CF (2009) TILLING in grass species. Plant Physiol **149:** 158–164

Wolters H, Jürgens G (2009) Survival of the flexible: hormonal growth control and adaptation in plant development. Nat Rev Genet **10:** 305–317

Zar J (2010) Biostatistical Analysis, Ed 5. Prentice-Hall, Upper Saddle River, NJ